ON DEPOSITS IN JET ENGINES

By Roland Breitweiser

Lewis Research Center
National Aeronautics and Space Administration
Cleveland, Ohio

INTRODUCTION

Deposits on the surfaces of jet engines may cause serious performance losses. The deposits may obstruct flow, increase frictional resistance, and distort carefully prearranged flow patterns in turbojets, ramjets, and rockets alike. Past examples are the deposits found on turbojet engine turbines and stators resulting from use of leaded gasolines or carbon-producing fuels.

The deposit problem is now aggrevated by the use of high-energy fuels. The high-energy fuels often achieve their improved impulse at the expense of elements that produce solid and liquid combustion products(1). Examples of these fuels are the boron hydrides now being considered for use in jet engines. Boric oxide is a combustion product that is either solid or a viscous liquid at many engine conditions. On a long flight, the amount of boric oxide formed in a jet engine may be 15 times the engine weight. It is not surprising that more attention is being given to deposition as fuels of this type appear.

In general, the troublesome surface deposits may exist in the form of hard granular solids, soft agglomerates, congealed liquids, viscous fluid films, or mixtures of each.

The surface residues may originate from: (1) combustion products that exist in the solid or liquid phase in the flame zone or in the subsequent parts of the engine, and (2) pyrolized products of incomplete combustion, including residues of metallic additives.

The manner in which the deposits contact surfaces may result from:

(1) Molecular diffusion of condensable vapors

(2) Diffusion of molecular clusters

(3) Impingement of large particles

(4) Runoff from upstream parts

The shape and size of the deposits are influenced by the physical state of the constituents of the deposits and the dynamic forces acting on them.

The loss in engine performance caused by the deposits is, of course, dependent on the type of engine and the particular engine component involved. Some generalizations of the effect of deposits are possible, since similar components are present in all jet engines.

These, then, are some of the factors that must be treated in a study of deposits on engine surfaces.

ORIGIN OF SURFACE RESIDUES

Condensable Combustion Products

One of the largest potential sources of deposits is from the combustion products that may be in the liquid or solid phase in the combustion zone, or from those products that may condense in the cooler static temperatures downstream of the combustor. The lower temperatures may arise from expansion of the working fluid or from contacting cool engine surfaces. Typical troublesome combustion products are: aluminum oxide, silicon oxide, boric oxide, magnesium oxide, or, in rockets, substances such as lithium fluoride.

If the temperatures and partial pressure of the combustion product are known, the first approximation of the physical state may be obtained from vapor pressures and melting-point data[3-5] of the type shown in figure 1. Some of the high-temperature data may be slightly inaccurate; for example, there is considerable scatter of the experimental boric oxide vapor pressure.

The vapor pressure data are based on equilibrium conditions and thus will not be directly applicable to the short residence times encountered in jet engines.

If the mechanism of deposition is to be understood, the physical state of the depositing constituent must be established. Admittedly, the potential deposit may be in many forms; however, the pathway to many deposits appears to be through the liquid phase. The liquid phase is usually produced from vapors that condense to form small molecular clusters that may eventually grow to liquid drops.

It is this liquid particle growth that has an important bearing on deposition, since the size of the particle defines the deposit mechanism, and the number of these particles defines rate of deposition.

The kinetics of particle growth is moderately well understood for relatively slow condensation periods in a system that has a continual replenishment of the condensing vapor of known physical properties. Unfortunately, these are not the conditions found in jet engines. Since the formation deposits are so strongly

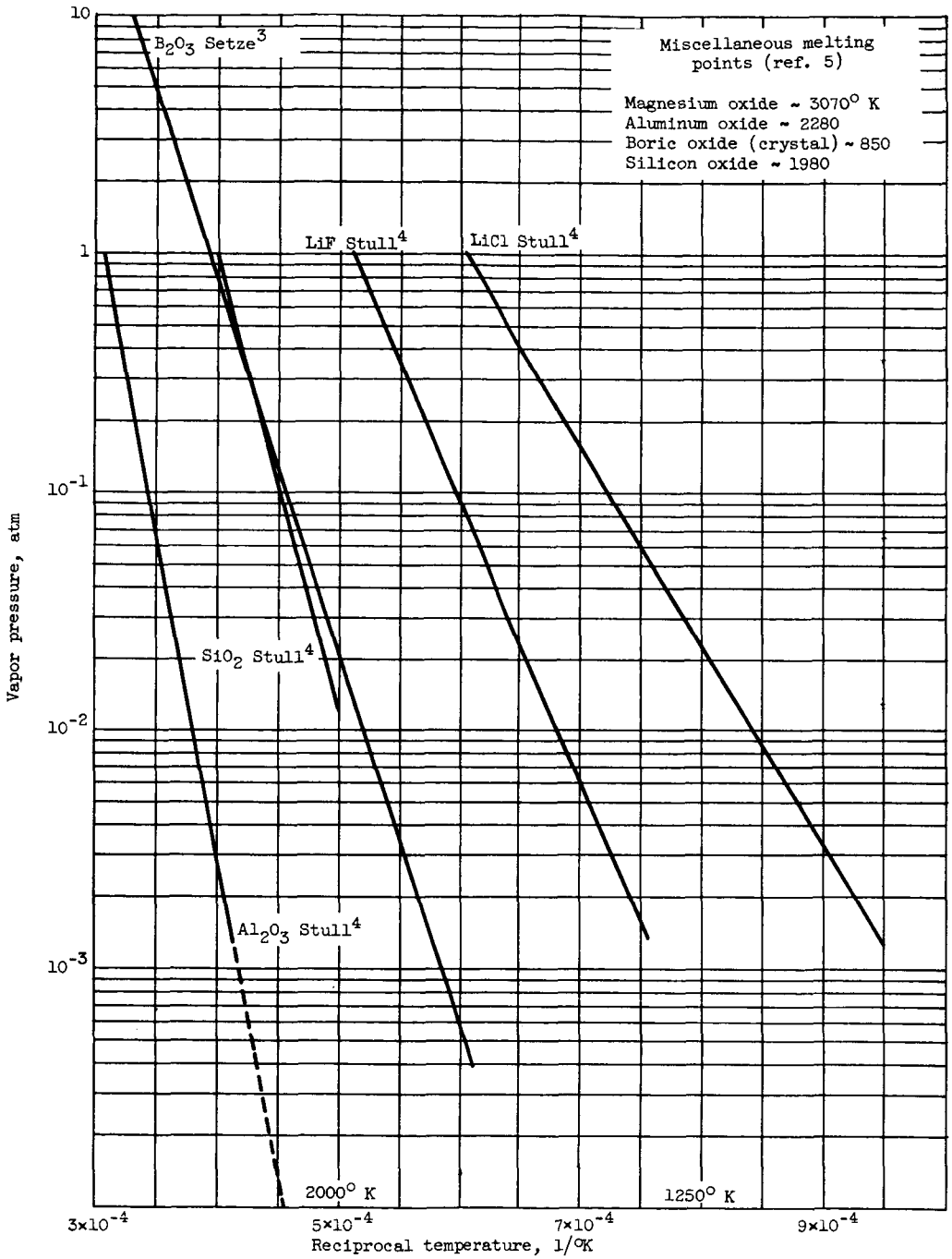

Figure 1. - Vapor pressure of some typical combustion products.

dependent on particle growth, some of the relations used to describe the growth will be presented herein. The particle growth relations will be reviewed in some detail, so that some of the limitations in use will become apparent. The material on particle

growth is partially based on two summaries of this field by Frenkel[6] and Stever[7].

The various relations used to describe the state of a condensible fluid may be classified as follows:

(1) Thermodynamic treatment based on equilibrium conditions (Frenkel[6], Helmholtz[8], Gibbs[9], Thomson[10]). These relations are applicable only for long residence times.

(2a) Pseudo-kinetic methods based on formation of critical size drops that serve as nuclei for particle growth (Volmer[11], Becker and Doring[12], Frenkel[6], Zeldovich[13], and others). Approaches of this type are best suited to moderate supersaturation and constant vapor pressure.

(2b) Refined kinetic methods that include particle growth by simultaneous heat and mass transfer to particles larger than the critical drop size (Oswatitsch[14]), and those methods that similarly treat the subcritical particle growth (Kantrowitz[15] and Probstein[16]).

(3) Approximate kinetic treatment for conditions of extreme supersaturation (Setze[19]).

Thermodynamic considerations. - The equilibrium state of a gas may be described in terms of free energy, equilibrium being defined as the condition were $d\bar{F} \rightarrow 0$. For the case of a liquid drop and the vapor surrounding it.

$$\bar{F} = N_V F_V + N_l F_l + 4\pi\sigma r^2 \qquad (1)$$

where

N_V number of vapor molecules

N_l number of liquid molecules

F free energy of particles at given temperature T and pressure p

σ surface tension

r radius of particle

Equation (1) may be rewritten without the surface tension term if the free energy of the particle is described in terms of the internal pressure of the drop.

At equilibrium ($d\bar{F}=0$), letting the total number of particles be constant ($N_V+N_l=C$),

$$F_V - F_l = 4\pi\sigma \frac{dr^2}{dN_l}$$

or

$$F_v - F_l = \frac{2\pi\sigma}{r} V_l' \tag{2}$$

where V_l' is the volume of a single molecule in liquid phase (continuum assumed). Frenkel[6] rewrites this equation by noting $dF = V\,dp$ and arrives at

$$\ln \frac{p}{p_\infty} = \frac{2\pi\sigma V_l'}{rkT} \tag{3}$$

where

k Boltzmann constant

p pressure surrounding the particle

p_∞ pressure of vapor in presence of an infinite liquid

T temperature

The same result may also be deduced by describing the energy required to evaporate a single drop (see Frenkel[6]).

As a drop becomes small, equation (3) indicates that the vapor pressure referred to the small drop is very high in comparison with the vapor pressure referred to an infinite liquid. Consider the case of drops of various sizes. The small drops will have a high vapor pressure, larger drops a lower vapor pressure. Vapor will tend to escape from the small drops more rapidly than from the large drops, causing a more rapid rate of disappearance of small drops. A molecular viewpoint is sometimes used to describe this phenomena: The surface molecules in the smaller molecular clusters have fewer bonds holding them together, the number reducing as radius decreases, so that the probability of escape from the small rather than the large drops is increased.

Although this treatment infers an unstable condition for any particular drop, the free-energy relations describe the most probable size distribution for groups of drops in a Maxwellian gas. Equation (1) may be written to describe the change in free energy of a group of vapor particles passing to the liquid phase:

$$\overline{F} - \overline{F}_o = \overline{\Delta F} = N_v F_v + N_l F_l + 4\pi r^2\sigma - (N_v + N_l) F_v \tag{4}$$

where $\overline{F}_o = (N_v + N_l) F_v$ is the free energy of the system at T and p when no drops are present.

There results

$$\overline{\Delta F} = - \frac{(F_v - F_l)}{V_l'} \frac{4\pi r^3}{3} + 4\pi\sigma r^2 \qquad (5)$$

Fluctuations in density exist in a gas. Thus, locally, in the higher density regions the thermodynamic potential for the liquid phase exists. Using the Gibbs relation to describe the number that exists in the variable density field gives.

$$N_g = Ce^{-\overline{\Delta F}/kT} \qquad (6)$$

where N_g is the number of drops containing g molecules in a gas of C molecules. Equation (5) is valid only when $N_g \ll C$. For conditions where N_g is an appreciable fraction of the total, terms analogous to the entropy of mixing must be included (see Frenkel[6], p. 383).

Equations (5) and (6) are the starting point of most particle growth expressions. Rewriting equation (5), treating the vapor as a perfect gas, gives

$$\overline{\Delta F} = - \frac{4\pi r^3 kT}{3V_l'} \ln \frac{p}{p_\infty} + 4\pi\sigma r^2 \qquad (7)$$

$$N_g = Ce^{-\left[-4\pi r^3 kT(\ln p/p_\infty)/3V_l' + 4\pi\sigma r^2\right]/kT} \qquad (8)$$

At equilibrium between liquid and vapor phase, $p = p_\infty$, the number of drops of dimension r is

$$N_g = Ce^{-4\pi\sigma r^2/kT} \qquad (N_g \ll C) \qquad (9)$$

if r is 6.1×10^{-8} cm, and $T = 1000^\circ$ K, the number of drops in 1 gram of water vapor is about 6.1×10^8.

At conditions of supersaturation where $\ln p/p_\infty$ is positive, $\overline{\Delta F}$ has the property of increasing with r to a maximum value and then decreasing for further increases in r, as can be seen from equation (8).

This value of critical radius, r, where $\overline{\Delta F}$ is a maximum may be determined from equations (1) and (2) by writing the free-energy equation for the critical drop where $dF/dg^* = 0$; there results $\Delta Fg = 4\pi\sigma r^{*2}/3$. It follows that

$$r^* = \frac{2\sigma V_l'}{kT \ln p/p_\infty} \qquad (10)$$

Treating the unsaturated vapor case first, equations (6) and (7) show the decreasing probability of the number of particles as r increases, since both terms of equation (7) are positive and are increasing with r. Small drops will form and grow in the

local regions of high density but, lacking the thermodynamic capacity for further growth, will disappear as they next experience local regions of lower vapor density.

Above saturation, $\overline{\Delta F}$ will increase with r to the critical drop size. The number of drops will decrease with increasing r, but a finite number of these critical drops will exist. A chance collision of the critical drop with a vapor molecule will increase the radius, decreasing $\overline{\Delta F}$ and increasing the probability of existence. At this condition there is no deterrent to further growth; the condition is unstable and has been described as the pathway of condensation. Frenkel[6] compares the $\overline{\Delta F}^*$ to an activation energy of condensation.

Vollmer[11] used the formation of critical drops to describe a condensation rate. His viewpoint was simply that the vapor would disappear from the system by the critical drop size route. So, by summing the total number of critical drops disappearing from the system, the condensation rate is established. Noting that only one molecule is required to move a drop past the critical size to the supercritical size, Vollmer wrote:

$$Q = g^* N^* \beta \tag{11}$$

where g^* is the number of molecules in a critical drop; N^* is the number of critical drops defined by equations (8) and (9); and β is a coefficient based on a simple kinetic expression describing the number of molecules striking the drop surface.

$$\beta = 4\pi r^{*2} \frac{p}{\sqrt{2\pi m k T}} \tag{12}$$

Frenkel[6], Becker and Doring[12], Zeldovich[13], and others have retained the concept of a critical drop size but have determined the condensation rates by another method. They note that, if a fixed drop size distribution is maintained, the evaporation from a drop must equal the condensation. Differential expressions that result in the evaluation of rate of evaporation as a function of stream conditions and drop size are then written. Knowing the rate of evaporation and the rate of condensation (assumed equal to the molecular condensation rate in Vollmer's expression), it is possible to solve for particle growth rates. The differential expressions for drop size require several approximations for their solution. A solution given in Frenkel[6] credited to Zeldovich[13] is

$$I = Ce^{-4\pi\sigma r^{*2}/3kT} \frac{p}{kT} \left[V_l' \sqrt{\frac{2\pi\sigma}{m}} \right] \tag{13}$$

where I is the rate of formation of supercritical drops. This expression is almost identical with the solution by Becker and Doring[12]. The corresponding equation of Vollmer's[11] was:

$$I = Ce^{-4\pi\sigma r^{*2}/3kT} \frac{p}{kT} \left[4\pi r^{*2} \sqrt{\frac{kT}{2\pi m}} \right] \tag{14}$$

The exponential is the same; however, the bracketed terms differ.

The value of the bracketed terms for water vapor at 300° K, supersaturated so $p/p_\infty = 2.718 \cdots$ is

$$[\quad] \text{ Zeldovich} = \left[3\times10^{-23}\sqrt{\frac{2\pi(70)}{m}}\right] = \frac{6.3\times10^{-22}}{\sqrt{m}}$$

$$[\ ] \text{ Vollmer} = \left[4\pi\times10^{-14}\sqrt{\frac{1.38\times10^{-16}}{2\pi m}}\,(300)\right] = \frac{100\times10^{-22}}{\sqrt{m}}$$

All conditions being equal, the Vollmer expression indicates a more rapid formation of supercritical drops. Comparison of the quantity in the bracket can be misleading, since the exponential is the dominating expression. The effect of the exponential will be discussed later.

The complete expressions for particle growth must include further growth past the critical drop size. The methods usually used are essentially similar to those of Oswatitsch[14]. Oswatitsch recognized that, when molecules condensed on a drop, the heat of condensation would raise the temperature of the drop. The mass (and energy) transfer to the drop was equated to the heat transfer to the surroundings. Thus, a vapor acceptance rate was defined. The equations were based on molecular flow for small particles, and continuum flow for the large. Provision for accommodation coefficients were included.

The expressions are:

$$r - r_o = \frac{1}{\mathscr{L}}\frac{Cp}{\rho_l}\sqrt{\frac{k}{mT}}\,(T_l - T)\tau \qquad \text{(Free molecule conditions)} \qquad (15)$$

where $\mathscr{L}$ is the heat of vaporization, and C is a constant including an accommodation coefficient; C usually is ≈ 1.

$$r - r_o = \sqrt{\frac{2k(T_l - T)}{\mathscr{L}\rho_l}}\,\tau \qquad \text{(Continuum conditions)} \qquad (16)$$

Many refinements to the critical drop size path for particle growth have been introduced in more recent years. Collins[18], Kantrowitz[15], and Probstein[16] have explored the time lag required in forming the "critical drop" resulting from a change in saturation pressure. Collins' solution of Frenkel's differential equation of drop growth results in a relaxation time equal to

$$\tau = \frac{kT}{4\gamma\beta}$$

where β is defined in equation (12) and

$$\tau = \frac{V_l' kT \ln p/p_\infty}{4\pi r^{*3}} \qquad (17)$$

Collins noted that solving the expression for water vapor at 0° C and a p/p_∞ of 4, the relaxation time is 1.4×10^{-6} second. Thus, if the conditions of equation (17) are satisfied, a very rapid supersaturation rate would be required for departure from the self-nucleation expressions of Zeldovich[13] and Becker and Doring[12].

Limitations of the "critical drop size" particle growth analysis. - As noted, the simple treatment of Vollmer was modified by Zeldovich and by Becker and Doring. A reduced supercritical drop formation rate resulted; but the difference between the two expressions can be easily masked by discrepancies in evaluating the exponential term. An example of the effect of the exponential (similar to Frenkel[6], p. 398) can be observed by the effect of the supersaturation ratio on the relative rate of formation of supercritical drops.

Supersaturation ratio, p/p_∞	Critical drop size, r^*, cm	$e^{-4\pi\sigma r^{*2}/3kT}$
2.718	10×10^{-8}	1.73×10^{-32}
7.4	5×10^{-8}	9.1×10^{-9}
20	3.4×10^{-8}	3.1×10^{-4}

The diameter of the critical drop does not vary appreciably, but the number of the drops undergoes a 10^{28} change.

The sensitivity of the growth rate to values of the exponential term has also been discussed by Stever[7]. In addition to the sensitivity to saturation pressure, Stever noted that the critical drop radius is a linear function of σ, the surface tension. Therefore, the number of critical drops and thus condensation rates are dependent on $e^{-K\sigma^3}$. A 26-percent error in surface tension may introduce a 10^5 error in condensation rate (at $p/p_\infty = 7.4$). The probable error will be greatest at conditions of large supersaturation, since the critical drop size is small at these conditions and the constant value of surface tension would not be expected to apply.

Head[19] suggests that the Tolman[2] values of surface tension be used; that is,

$$r = \frac{1}{1 + (2\delta/r)}$$

where $\delta \approx r/2$ of molecule.

Bogdonoff and Lees[21] analogize the binding energy drops to that of metal crystals. With this and calculations of Reed[22], they suggest that the binding energy approximates $E_\infty/6$ up to 8 molecules, finally approaching normal binding energies at clusters of 20 or more molecules. In the case of some of the condensable fluids such as boric oxide, further complications arise in that the condensable fluid may react with the other constituents present. There is strong evidence that water vapor reacts with boric oxide, (B_2O_3) to form anhydrous boric acid (HBO_2). Thus, the pathway to aggregation in this case can be influenced by competing chemical reactions.

As stipulated by Collins[18], the expression for relaxation time is valid only "in absence of complicating effects" and had greatest utility for the particular cases he was exploring. Kantrowitz[5] and Probstein[16] analyzed relaxation times and were interested in calculating rates of heat liberation from highly supersaturated, rapidly expanding vapors. The Kantrowitz analysis emphasized the heating of the growing subcritical drops in a manner somewhat analogous to the Oswatitsch treatment of supercritical drops. The local vapor pressure of the heated drop was altered, thus changing the relaxation times.

Kantrowitz accepted the lack of information on the various accommodation coefficients and thermodynamic states in the small molecular clusters and restricted the scope to comparison of the trends of the analysis to experimental data. He hypothesized that the time to move from saturation to condensation shock varies with the 4^{th} power of the degree of supersaturation. This was substantiated by experiment and thus lends some credence to his stressing the effect of particle heating on the kinetics of early growth processes. The particle heating will increase relaxation time and thus reduce the number of critical drops formed.

Further problems in the use of the "critical drop size" approach exist: In large amounts of supersaturation, the expression "C" (eq. (6)) and (13)) must be modified, for no longer is $N_l \ll N_g$. The solutions of the expressions then require a tedious iteration procedure.

It should be noted that the Zeldovich, Becker and Doring, and Vollmer expressions are based on a constant replenishing of vapor; whereas, in many cases the amount of condensable fluid is constant, so that the vapor is depleted during the particle growth process. This, of course, will have a major effect on the rate of particle growth. The complete analytical expressions including this effect are quite complex; however, an expression that illustrates the effect of vapor disappearance can be developed fairly simply.

In treating the case of a large amount of supersaturation (particles highly subcooled), assume that the number of vapor molecules striking the surface can be defined as

$$- \frac{dn_v}{d\tau} = \pi D^2 \mathscr{D}(n_v)$$

where $\mathscr{D}$ is a diffusion coefficient. Vapor concentration is assumed zero at surface of the drop. Noting that the rate of vapor condensation is

$$- \frac{dn_v}{d\tau} = \frac{d(V)}{V_l' d\tau} = \frac{\pi}{2} D^2 \frac{dD}{d\tau} \frac{1}{V_l'}$$

when $n_{v,\tau=0}$ is the number of molecules of condensable fluid, the equation for particle growth is, if the number of liquid particles is held constant,

$$n_l \frac{1}{V_l'} \frac{\pi D^2}{2} \frac{dD}{d\tau} = n_l \pi D^2 \left(n_{v,\tau=0} - \frac{\pi D^3}{6 V_l'} n_l \right) \mathscr{D}$$

or

$$d\tau = \left[\frac{dD}{n_{v,\tau=0} - \frac{\pi D^3 n_l}{6 V_l'}} \right] \frac{1}{2 \mathscr{D} V_l'}$$

There results:

$$\tau_2 - \tau_1 = \left[\frac{1}{6a^2} \ln \frac{a^2 + aD + D^2}{a^2 - 2aD + D^2} + \frac{1}{a^2 \sqrt{3}} \tan^{-1} \frac{(2D + a)}{a \sqrt{3}} \right] \frac{3}{\pi (n_l) \mathscr{D}}$$

where

$$a = \left(\frac{6 n_{v,\tau=0} V_l'}{\pi n_l} \right)^{1/3} \qquad (17)$$

The equation predicts extremely rapid growth of drops during the time immediately after the critical drops are formed, followed by slow growth. The slow growth is, of course, the result of depletion of vapor.

Numerical examination of this equation and of equation (13) indicated one further limitation of the critical drop size approach. At conditions of large supersaturation, the population density of critical drops becomes large. When a fixed amount of condensable fluid exists, the vapor is quickly depleted. Thus the probability that a cluster of drops will collide with another cluster increases. Growth through cluster collisions may then take place.

The probability of collision of one class of molecules, class 1, with another, class 2, can be approximated by the following equation (Jeans[23]):

$$\text{Collision probability of } 1 \text{ with } 2 = \sqrt{\pi}\left(\frac{n_2 S_{12}^2}{m_2 C_1}\right) 2kT \left[\Psi C_1 \sqrt{\frac{m_2}{2kT}}\right]$$

where C is velocity of the sweeping particle and S is the sum of the particle diameters.

The bracketed expression is a complex function containing the error function. However, if we examine only the case of a single velocity, that being the most probable velocity, and assume the collision cross section is proportional to $(g_1^{1/3} + g_2^{1/3})^2$, the expression may be evaluated easily.

The relative probabilities of collisions of several sets of particles are shown as follows for conditions of constant temperature and constant particle density. (Note: Probability is proportional to density.)

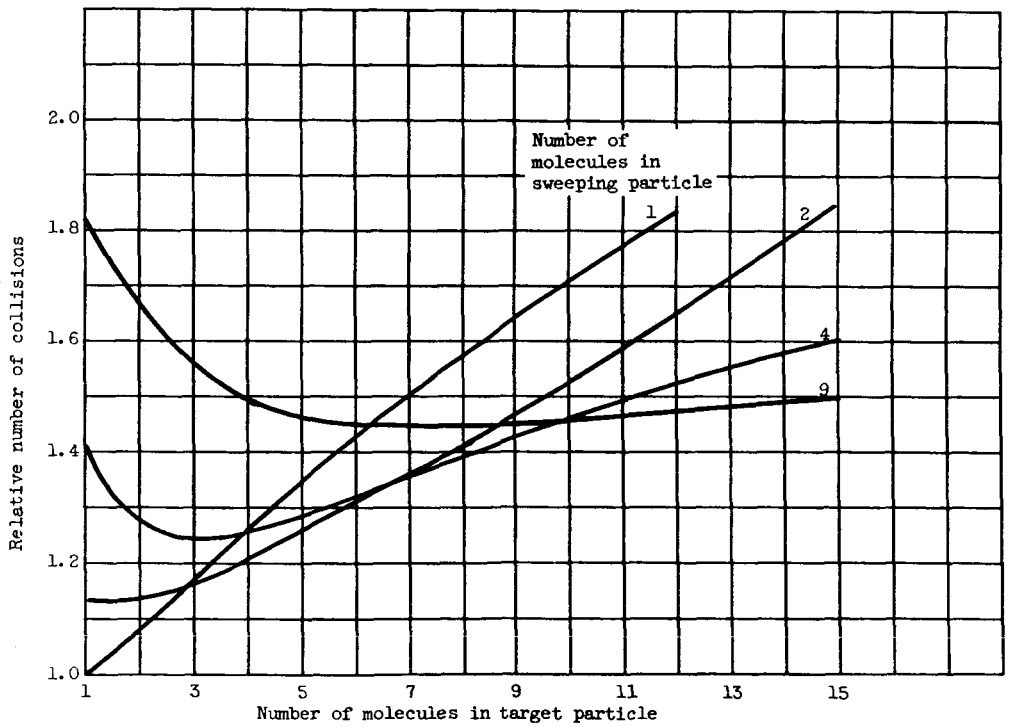

Figure 2. - Effect of particle size on collision activity.

The cumulative collision activity of each of the molecular clusters with all sets considered is about the same.

Figure 2 serves only to indicate that collision activity of the larger particles must be included in determining terminal drop sizes when the particle density of the larger particles become significant.

An additional factor that must be observed is the ambiguity of the term β (eq. (12)) which describes the number of vapor molecules contacting the drop. The growth expressions should be modified to properly account for the effect of particle size, diffusion of multiple molecular clusters, and the effect of other gases present. Diffusion equations of the type developed in a later section can be used as a basis of modification of the original diffusion equations. The usual Knudsen number relations can be used to describe when the diffusion equations should be altered from the simple kinetic model.

An approximate expression for large amounts of supersaturation. - Setze[17] developed analytical expressions for particle growth based on the growth activity of multimolecule clusters. The analysis supported his experimental data dealing with the growth of boric oxide particles at simulated jet engine conditions. The supersaturation was severe for all conditions, amounting to 1800° R below the saturation condition. Some of the major assumptions in the analysis were:

(1) At the conditions of high supersaturation, all collision of the particles results in the formation of larger particles.

(2) Particles are spherical.

(3) At any time τ after supersaturation, a narrow particle size range exists.

(4) The particles act as large gas molecules.

The unique assumption is (3), which infers that the growth occurs through collisions of equal size particles, a like-on-like process. Justification for this assumption was based on the experimental observation that a very narrow size range of particles existed at the various stations downstream of the flame zone (various growth times). Also, the work of Longstroth and Gillespie[26] was cited by Setze; their work dealing with the aging of smokes indicated uniformity of terminal sizes and inferred uniformity of intermediate sizes.

The basic analytical expression used by Setze,

$$\frac{d\theta}{d\tau} = \frac{4}{3}\pi N_p D_p^2 u_p \qquad \begin{matrix}\text{(Number collisions} \\ \text{per unit time)}\end{matrix} \qquad (18)$$

which integrated from time zero to time τ holding the initial number of condensable molecules constant, results in

$$D_{g,\tau}^{5/2} - D_0^{5/2} = (k\tau) \qquad (19)$$

where

$$k = \left(\frac{V_l}{V_g}\right)\sqrt{\frac{RT}{\rho_l}}\,(20.56\times10^{-12})$$

the quantity V_l/V_g is the initial relative volume of condensable liquid to gas; T is in ^{o}K; and ρ_l is in grams per cubic centimeter.

The factors influencing this type of growth can be seen directly from the kinetic growth equation, noting that:

Number of particles per unit volume $\sim \frac{1}{D^3}$

Velocity of particles $\sim \frac{1}{D^{3/2}}$

Collision cross section $\sim D^2$

Then,

$$\frac{d\theta}{d\tau} = \left(\frac{1}{D^3}\right) \quad \left(\frac{1}{D^{3/2}}\right) \quad (D^2)$$

Concentration Velocity Cross section

Also,

$$\frac{d\theta}{d\tau} = \frac{1}{V_p}\frac{dV}{d\tau} = \frac{\pi}{2V_p}D^2\frac{dD}{d\tau} = \frac{3}{D}\frac{dD}{d\tau}$$

$$\frac{dD}{d\tau} = \frac{k'}{D^{3/2}}$$

Integrating and letting $V_p = 0$ at $\tau = 0$,

$$D \sim \tau^{2/5} \qquad (20)$$

One of the predominant terms is the concentration $1/D^3$. The reduction in number of particles as the particles grow, strongly influences terminal size. A pleasant characteristic of the equation is the insensitivity of the expression to drop size in the residence times normally encountered in jet engines. The basic equation exhibits a 0.4-power dependence of diameter on time. In the case of a typical condensable product, a very rapid growth in the 0 to 2 millisecond range is indicated, followed by relatively slow growth rates occurring in the 2 to 30 millisecond range. This can be seen in figure 3, where particle diameter is plotted as a function of residence time. The value k (eq. (19)) corresponds approximately to values encountered in the use of boron hydride fuels at jet engine conditions. Typical residence times of jet engines are indicated.

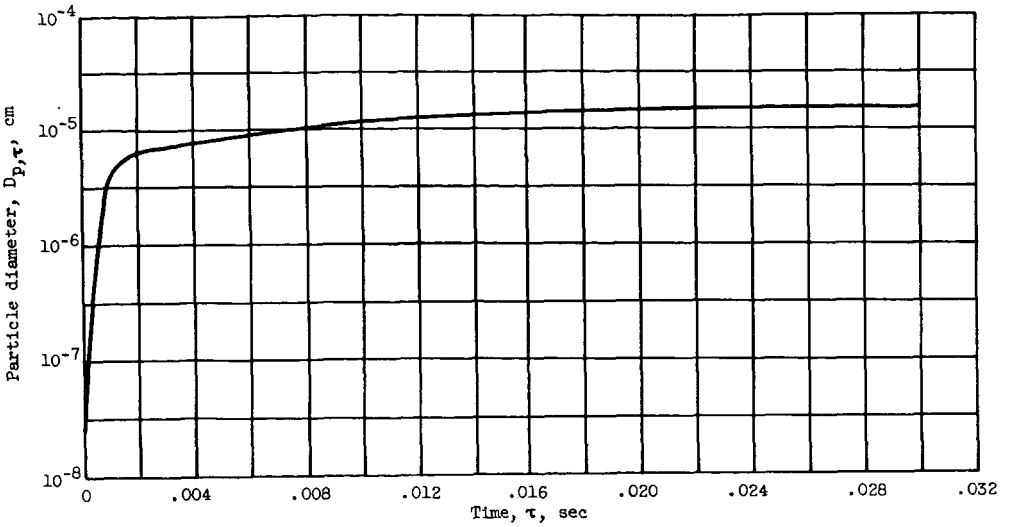

Figure 3. - Theoretical particle diameter as a function of growth time for $K = 4 \times 10^{-11}$.

The effect of kinetic growth factors such as effective collision cross section can be examined directly in relations of the simplicity of equation (20). For example, if the particle collision cross section were only 50 percent effective, the drop size would be reduced 26 percent. Since the greatest uncertainty in particle growth factors exists during the early periods when the particle is small, these effects may have small influence on the terminal size if: (1) High supersaturation exists, and (2) relatively long residence times are considered.

Setze's equation (19) and equation (17) based on condensation nuclei are similar in that both recognize the diminution of condensable vapor and thus have rapid early growth and very small size change in the latter time periods. Errors in assumptions during early growth periods may not affect terminal drop size if sufficient time for growth is present. The cases of greatest uncertainty occur in the short residence times, as might be encountered in sudden expansion of a condensable fluid in a nozzle. Fortunately in deposition studies we are usually interesested in the case where particle growth has occurred prior to the nozzle.

Experimental data on drop sizes. - Much of the drop size data for the residence time range of jet engines has been obtained by the light scattering technique. An example of this method is given in reference 7. The relations between analytical relations (based on critical drop theory) and measured drop sizes can be construed to give reasonable agreement (Stever[7]).

Rather than enumerate all the literature on measured and estimated drop sizes, a more detailed review will be presented of the particle measurements made by Setze[17].

The particle growth experiment was conducted in a 4-inch-diameter combustion tunnel using pentaborane-air combustion products. The combustor resembled a flat-flame burner. At several stations downstream of the burner, portions of the combustion products were sampled These samples were rapidly chilled in a spray of liquid nitrogen. The solidified boric oxide particles were then collected by an electrostatic precipitator. The size was determined by electron microscopy. The following range of conditions were covered: 1 to $1\frac{1}{2}$ atmospheres pressure, 1260° to 2260° R temperature, 2.5 to 30 milliseconds growth time, and 1800° to 2200° R supercooling.

Approximately 50 particles were counted in each run; and the relatively low number was considered adequate, since in each run a fairly small size distribution existed. A typical particle size range was 1.0×10^{-5} to 1.6×10^{-5} cm, the maximum number occurring at 1.3×10^{-5} centimeters.

Over the entire range of conditions covered, the average particle diameters fell between 1.1×10^{-5} and 1.46×10^{-5} centimeter.

The small size range of particles in any one sample partially validated Setze's assumption of growth in uniform size range. The probable error between calculated and experimental values was about ±34 percent, thus indicating reasonable agreement with the analysis.

The role of foreign-body condensation nuclei. - The subject of condensation and growth on foreign particles has not been emphasized. In order for any appreciable amount of condensation to occur, the number of particles must approach the number of critical drops present in supersaturated vapor. The number of dust particles in air is normally insignificant in comparison with the number of self-nucleated particles.

An example that may be construed as an exception is when combustion products contain two condensable products, such as with aluminum-boro-hydride fuel. The combustion products are aluminum oxide, boric oxide, and water vapor. Both aluminum oxide and boric oxide are condensable at jet engine conditions. The aluminum oxide would condense first since the vapor pressure is about two orders of magnitude less than that of boric oxide. The boric oxide would have aluminum oxide nuclei to build upon, and thus boric oxide growth would be accelerated. Although this accelerated growth method has not been confirmed experimentally, an analogous observation was made by Arthur and Nagamatsu[25]. Arthur observed that small amounts of water vapor and carbon dioxide accelerated the occurrence of the condensation of nitrogen and oxygen in hypersonic tunnel tests; they attributed this acceleration to nucleation by the trace constituents.

The condensation rates and particle growth of multicondensable component systems should be solvable by the judicous applications of analytical expressions, such as equations (17) and (19).

Summary regarding growth of particles from condensable combustion products. - Reviewing the limitations, it appears that particle growth equations of critical drop size type may be used at conditions of moderate supersaturation. At these conditions, if the amount of condensable fluid is fixed, equations (13) and (15) must be altered to correct for the change in vapor pressure. At conditions of large amounts of supersaturation, no generalizations can be made. The effect of changes in surface tension, subcritical drop heating, vapor depletion, and probability of multimolecule collision must be considered for the particular fluid considered. Unfortunately, the effect of high supersaturation must be considered in each part of the parent equations.

At the conditions of high supersaturation, approximate solutions similar to those of Setze[17] would appear to be as reliable as any, and have the merit of simplicity. The sluggish terminal growth caused by the consumption of small particles and vapor molecules seems to compensate for lack of thermodynamic and kinetic information.

Experimentally, most particles formed by condensation in jet engine gas streams appear to be in the submicron range because of the residence times involved.

Deposits Resulting From Incomplete Combustion

It is difficult to quantitatively discuss the formation of depositable materials caused by incomplete combustion. Each fuel, each system has its own peculiar tendency to produce products that may form surface residues. Solid rockets may contain fuels, binders, or additives that do not react completely and thus may potentially collect on the nozzle surfaces. Slurries of metals may be used in ramjets. The metal in the slurry may melt and impinge on engine surfaces before combustion is complete. More commonplace fuels such as the hydrocarbons may form coke or smoke under certain combustor operating conditions.

Of all the cases, the hydrocarbon-air systems has received the greatest attention and will be used to illustrate sources of deposits through incomplete combustion.

A survey of the smoke and coke formation in the combustion of hydrocarbons has recently been published by Schalla and Hibbard[26] and is used as a nucleus of this discussion. Smoke is defined as the solid suspended in the combustion gases, and coke as the material adhering to combustor walls. Smoke is a combination of carbon, hydrogen, and oxygen; a typical analysis is 96.2 percent carbon, 0.8 percent hydrogen, and the remainder is believed to be oxygen (ref. 27). Coke varies from soft, light, fluffy material to hard vitreous deposits. Again, the composition is predominantly carbon with small fractions of hydrogen, oxygen, and perhaps traces of sulfur.

The general mechanism of smoke formation presented by Schalla[26] is:

(1) Some hydrogen atoms are removed from the fuel by thermal processes. The atoms in turn further dehydrogenate the fuel molecule.

(2) These fuel molecules continue to decompose to smaller molecules and molecular fragments, and then undergo a simultaneous polymerization and dehydrogenation to form smoke.

The preceding mechanism is consistent with smoking tendency of fuels (aromatics > alkynes > olefins > n-paraffins).

The terminal size of smoke particles is dependent on the initial polymerization steps, followed by particle agglomeration steps similar to those discussed in liquid droplet growth. The mechanism of growth is confused by lack of knowledge of the effectiveness of particle collisions. Many indications point to submicron particle terminal sizes for the true smokes.

The mechanism for coke formation may be as follows: When fuel sprays impinge on hot walls, the less volatile fuel fractions may indulge in liquid phase cracking. The degraded fuel fractions may be accelerated to the semisolid state by the presence of oxygen, since oxygen is known to accelerate formation of high-molecular-weight asphaltic compounds.

The "softness" of the coke is assumed to be dependent on the amount of smoke ensnared in the liquid phase of the various coke-forming steps.

Factors noted in smoke and coke formation are:

(1) Smoke and coke are formed in fuel rich regions.

(2) Increasing pressure increases carbon forming tendency.

(3) Fuels vary in their tendency to smoke and coke which is related to the ease of hydrogen atom removal, compared with carbon bond stability.

Many of the features of petroleum fuel smoke and coke formation are consistent with other fuels.

Fuel-rich zones in combustors may produce degraded solid-fuel products. Fuels that exhibit this tendency will be those containing elements that may exist in the solid form, and also those whose partially oxidized fuel compounds exist in the solid form. Examples of fuel elements that may be in solid or liquid form are fuels containing boron, aluminum, magnesium, and carbon. Higher molecular weight compounds, with hydrogen and/or oxygen, of each of the elements may also encounter conditions of liquid or solid phase at many of the engine conditions. Impingement of these fuels on combustor walls, or combustion in excessively rich zones, in a local or gross sense may induce serious deposition. Figure 4 compares an extreme case of coke formation in a turbojet combustor

using hydrocarbon fuel to a combustor using a boron hydride fuel. Both suffered from fuel impingement, generally enriched fuel zones, and fuels susceptible to fuel degradation.

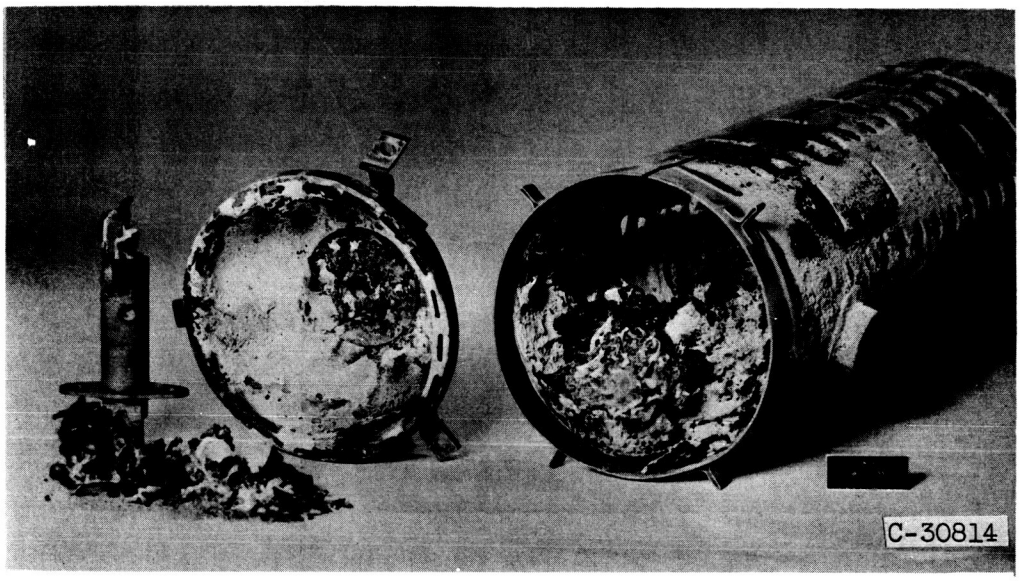

Deposits resulting from the use of a boron hydride fuel

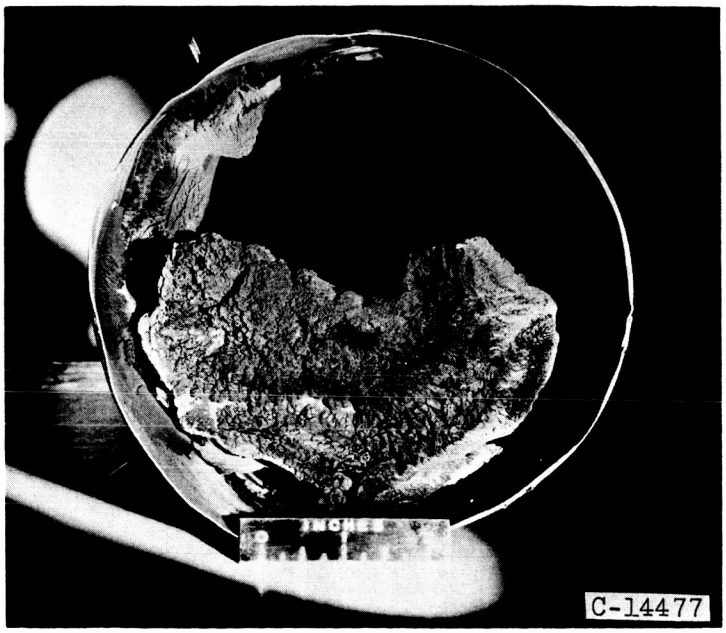

Deposits resulting from the use of a petroleum fuel with strong coke forming tendencies.

Figure 4. - Examples of severe combustor deposits.

MECHANISM OF SURFACE DEPOSITION

The mechanism of surface deposition is arbitrarily divided into:

(1) Deposition controlled by particle diffusion (particles less than 1/2-micron diameter)

(2) Deposition by impact of large particles, 5-micron diameter and greater

This division seems justified, since most particles are formed by the following methods: (a) liquefaction (or solidification) of a condensable constituent in the main gas stream, (b) poorly atomized and thus unburned fuel sprays, and (c) particles formed when liquid films on engine surfaces are blown back into the gas stream. The particle growth relations presented earlier indicate that the residence time available for the condensation of combustion products (a) limits particle size to the submicron range. The dynamic forces available for atomization (b and c) produce particles sizes larger than 5 microns. (The atomization of liquid film is discussed in a later section of this article.)

Diffusion of Vapors and Molecular Clusters

Diffusion coefficients. - The diffusion relations for a condensable vapor in a mixture of gases are quite complex. The rigorous equations and some of the simplifications are presented as follows: (Eqs. (20) to (25) are from unpublished notes by R. Brokaw[28], in which he reviews recent contributions in the field of diffusion by Hirschfelder and Curtiss[29-30] and Buddenberg and Wilke[31].)

The diffusion coefficient for a vapor, i, in a mixture of gases contining υ components can be found from

$$D_{im} = \frac{1 - x_i}{\sum_{\substack{k=1 \\ k \neq i}}^{\upsilon} \frac{x_k}{D_{ik}}} \tag{20}$$

where x is mole fraction, and

$$\mathscr{D}_{i,k} = \frac{2.628 \times 10^{-3}}{p D_{i,k}^2 \Omega_{i,k}^{1,1}} \sqrt{\frac{T^3 (M_i + M_k)}{2(M_i M_k)}} \tag{21}$$

where $\mathscr{D}$ is in square centimeters per second, T is given in °K, M is the molecular weight, and D, molecular diameter, is in angstroms.

The quantity Ω describes the effective collision cross section and is the function of kT/ϵ (ϵ, energy of the potential wall, ref 30). Values of Ω are given in Hirschfelder and Curtiss[30] for many molecules of interest. Values may be estimated for nonpolar gases from critical point data.

The current indefiniteness of the potential energy variations and collision diameters of clusters of molecules makes the use of the refined diffusion equations a questionable luxury.

As a first approximation, the diameter of molecular clusters may be based on equivalent rigid spheres. The diffusion coefficient for a binary system then reduces to

$$\mathscr{D}_{12} = \frac{3}{8\sqrt{\pi}} \frac{kT}{pD_{1,2}^2} \sqrt{\frac{kT(m_1 + m_2)}{2m_1m_2}} \tag{22}$$

where D is in centimeters and m is mass of particle. If 1 refers to the particle and 2 to the medium where $m_1 \gg m_2$ and $D_1 \gg D_2$, the equation reduces to

$$\mathscr{D}_{12} = \frac{3}{2\sqrt{\pi}} \frac{kT}{pD_1^2} \sqrt{\frac{kT}{2m_2}} \tag{23}$$

For still larger particles, the viscous effects of the fluid appear. The diffusion coefficient in this range is described by the Einstein equation.

$$\mathscr{D}_{12(\text{viscous})} = \frac{kT}{3\pi D_1 \mu} \tag{24}$$

Combining gives

$$\mathscr{D}_{12(\text{viscous+molecular})} = \frac{kT}{3\pi\mu D_1} \left(1 + \frac{\mu}{pD_1} \frac{9}{2} \sqrt{\frac{\pi}{2}} \sqrt{\frac{kT}{m_2}}\right)$$

Considering the gaseous medium as rigid spheres

$$\mu = \frac{5}{16\sqrt{\pi}} \frac{\sqrt{mkT}}{D^2}$$

there results

$$\mathscr{D}_{12} \approx \frac{3}{2\sqrt{\pi}} \frac{kT}{pD_1^2} \sqrt{\frac{kT}{2m_2}} \left(1 + \frac{pD_1D_2^2}{kT}\right) \tag{25a}$$

and

$$\mathscr{D}_{12} \approx \frac{kT}{3\pi\mu D_1} \left(1 + \frac{kT}{pD_1D_2^2}\right) \tag{25b}$$

Equation (25a) has been written as a molecular diffusion equation corrected for viscous effects. Whereas (25b) has been written as a molecular correction to the continuum viscous equation. Both are reliable in the extremes. It is interesting to note (25) introduces at most, a 20 percent variation from the currently accepted slip correction to the Einstein equation.

Thermal diffusion of vapors and molecular clusters. - Diffusion of particles in the presence of a temperature gradient introduces the forces of thermal diffusion. The forces of thermal diffusion for vapor molecules require a careful evaluation of the interaction potentials (von Kármán[32]). In the case of hard molecules, the large tend to migrate to the cold surfaces.

Chapman[33] suggests that the forces of molecular thermal diffusion will have a small effect on the over-all diffusion rate at conditions corresponding to the jet engine conditions considered herein. For an exact treatment of the forces of thermal diffusion, reference 30 is suggested.

Molecular clusters in a temperature gradient will be acted on by the gaseous particles in a manner analogous to thermal diffusion of large molecules.

Cawood[34] describes this effect on the motion of smoke and dust particles in a temperature gradient.

Cawood's equation is:

$$\text{Driving force} = -\frac{\rho}{2}\left(\frac{\partial T}{\partial y}\right)\frac{L}{T}\pi r^2 \qquad (26)$$

L is mean free path

where all terms are referred to gas stream, excluding the particle radius r.

Smith[35], in investigating equation (26), concludes that for highly cooled turbines mass diffusion will be most strongly augmented by the thermal diffusion when particle diameters are between 0.5×10^{-5} to 5×10^{-5} centimeter.

Mass transfer relations. - Treating a mixture of gases as a single gas, a binary mass flow equation for vapor may be written as

$$\frac{dx_1}{dy} = \frac{RT}{\mathscr{D}_{12}p}(x_1w_2 - x_2w_1) \qquad (27)$$

where w is mass flux (moles/(cm^2)(sec)). The case of greatest interest in deposition is diffusion through a stagnant film; in this case, $w_2 = 0$ and, since $x_2 = (1 - x_1)$,

$$w_1 = \left(-\frac{1}{1 - x_i}\right)\frac{\mathscr{D}_{12}P}{RT}\frac{dx_1}{dl} \qquad (28)$$

A more refined flux equation for diffusion through multicomponent stagnant stag mixtures is

$$w_i = -\frac{p}{RT}\frac{1}{\left[\sum_{k\neq i}^{n}\frac{x_k}{\mathscr{D}_{i,k}}\right]}\frac{dx_i}{dy} \qquad (29)$$

where v are the components in the static film. When $x_i \ll 1$, the expression may be written as

$$w_i = - \mathscr{D}_{i,m} \frac{p}{RT} \frac{dx_i}{dy}$$

$D_{i,m}$ is as defined in equation (20).

Using similarity relations, the equations of momentum transfer can be transformed into heat or mass transfer, thus mass transfer relations can be obtained for cynamic systems. Eckert[36] suggests that the Nusselt number for heat transfer can be transformed to mass transfer by replacing the Prandtl number by the Schmidt number and replacing thermal conductivity, λ, by the diffusion coefficient:

$$\frac{hl}{\lambda} = f(Re,Pr)_{heat} \quad \text{equivalent to} \quad \frac{h\mathscr{D}l}{\mathscr{D}} = f(Re,Sc)_{mass}$$

This same substitution often appears in the Stanton number form using the coefficient of friction C_f:

$$St = f(C_f,Pr)_{heat} \quad \text{equivalent to} \quad St_{\mathscr{D}} = Sh = f(C_f,Sc)$$

Sh is the Sherwood number.

An example of the resulting equation for mass transfer to a flat plate with laminar flow is:

$$St = \frac{C_f}{2} (Pr)^{-2/3} \quad \text{or} \quad Sh = \frac{C_f}{2} (Sc)^{-2/3} \tag{30}$$

$$\frac{h\mathscr{D}}{u} = \frac{0.332}{\sqrt{Re}\ (Sc)^{2/3}} \tag{31}$$

this relation can be directly transformed into the equivalent N Nusselt form to give:

$$\frac{h\mathscr{D}l}{\mathscr{D}} = 0.332 \sqrt{Re}\ (Sc)^{1/3} \tag{32}$$

The equations for mass transfer in laminar flow are then

$$\frac{dn}{d\tau} = \frac{(0.332)u}{\sqrt{Re}\ (Sc)^{2/3}} A \frac{dn}{dy} \tag{33}$$

or

$$\frac{dn}{d\tau} = 0.332 \sqrt{Re}\ (Sc)^{1/3} \frac{A}{l} \frac{dn}{dy} \tag{34}$$

The deposition rates of a condensable vapor can be compared with rates of deposition of various size molecular clusters by the use of equations (33) or (34) for the case of (1) constant number of condensable molecules, (2) constant Reynolds number, and

(3) equivalent mass concentration (vapor and particle concentration zero at wall). The results are presented in figure 5:

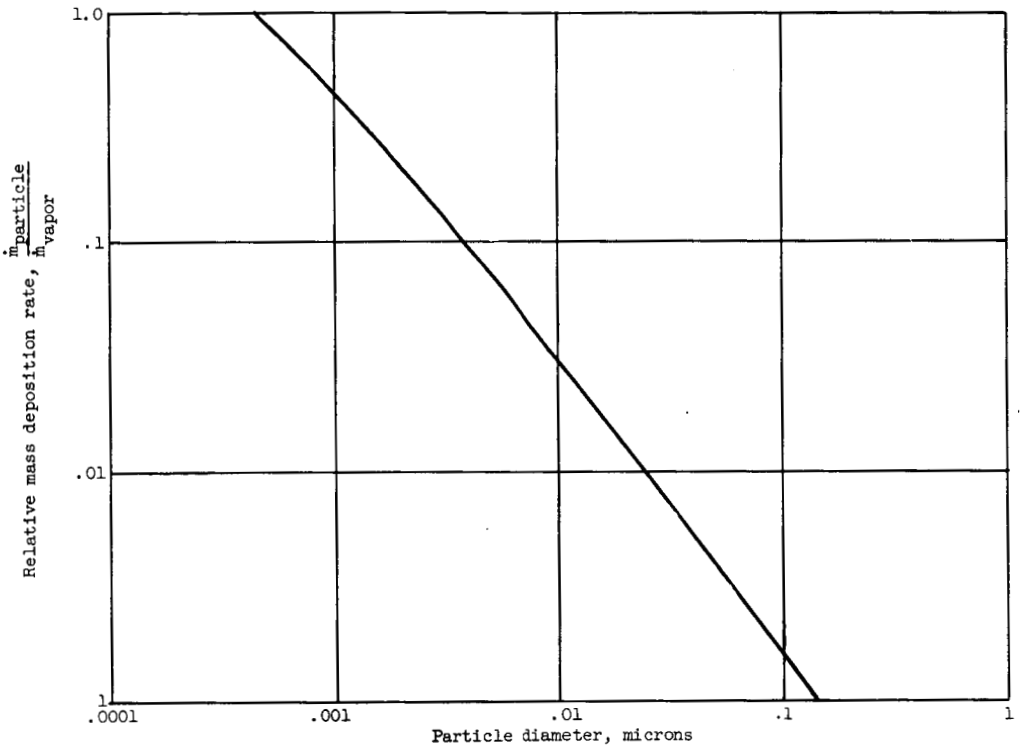

Figure 5. - The effect of particle diameter on rate of deposition.

The deposition rate of the molecular clusters in the size range expected in jet engines is several orders of magnitude less than that of vapor. Some questions as to the validity of these relations may exist for the particles, since Schmidt numbers of 10^5 are approached for 0.1 micron particles at realistic conditions. However, it is felt that, for laminar flow, the trends indicated are real.

The simple substitution inferred in equation (30) is not proper in turbulent flow at high Prandtl or Schmidt numbers because of the dominance of eddy diffusivity. Reichart[37] and Metzner and Friend[38] have developed relations that allow for the increasing importance of eddy diffusivity at these conditions. Metzner and Friends equation in Stanton number form is:

$$St = \frac{C_f/2}{1.2 + (Pr - 1)b'\sqrt{C_f/2}}$$

and for mass transfer,

$$Sh = \frac{C_f/2}{1.2 + (Sc - 1)b\sqrt{C_f/2}} \qquad (35)$$

where b' is the Reichart b' function and is defined as

$$b' = \int_0^{U/u'} \frac{q_{\text{molecular flow}}}{q} \, du^+ \qquad (36)$$

In effect, b' expresses the ratio of molecular flux to total flux averaged over the turbulent boundary layer.

Values of b' are presented in reference 38 for Schmidt numbers up to 3000. The design equation (pipe flow) recommended is:

$$\underset{(Sc<3000)}{Sh} = \frac{C_f/2}{1.2 + 11.8\sqrt{C_f/2}(Sc - 1)(Sc)^{-1/3}} \qquad (37)$$

Experimental results. - Setze[39] measured the deposition rates on a surface immersed in the combustion products of pentaborane and trimethylborate methanol azeotrope. The test conditions encompassed temperatures from 1200° to 1900° R, pressures from 1.0 to 1.5 atmospheres, and boric oxide concentrations from (2.7 to 5) $\times 10^{13}$ particles per cubic foot. The deposition rates were measured by operating the combustor for a fixed period of time and measuring the amount of boric oxide congealed on the surface of a flat plate.

The experimental results of Setze were analyzed first to determine an approximate Schmidt number. Equation (19) was used to estimate particle size. A diffusion coefficient, and thus a Schmidt number, was then calculated for this particle size. The Schmidt numbers varied from (0.4 to 1.4)$\times 10^5$. Cursory application of these Schmidt number results to a transport equation, using the relations of equation (37), gave values of deposition rates about 3 orders of magnitude less than the observed rate. This result was not surprising in view of the abnormally high Schmidt numbers. It is to be expected that the molecular flux of the large particles is small compared with the eddy flux. In essence the term b' in equation (35) might be expected to approach zero at Schmidt numbers of 10^5. The deposition rates were calculated by equation (35) modified to flat plate form and b' was set equal to zero. The resulting equations were:

$$Sh = \frac{0.074}{2(Re)^{0.2}} \qquad (C_f \text{ based on smooth flat plate data})$$

$$\frac{dn}{d\tau} = (Sh)u \frac{dn}{dl}$$

The particle concentration was assumed to be zero at the wall. The results are presented in figure 6.

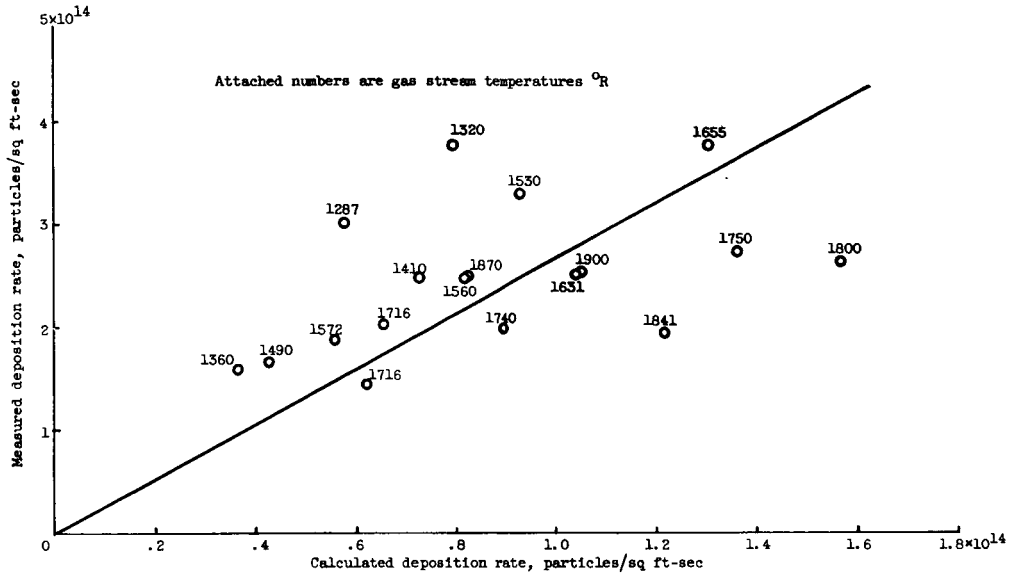

Figure 6. - Comparison of analytical and experimental boric oxide deposition rates.

The agreement between experimental and calculated values is good. Better agreement is possible if the coefficient of friction is juggled to account for the surface roughness caused by deposits of boric oxide. It is interesting to note that gas temperature causes a consistent deviation of the data. The uncooled flat plate temperature was roughly proportional to the gas stream temperature. It would be expected that the deposits would be thicker and rougher at the lower temperature conditions. Thus, the deviations in measured rate are in accord with variations in temperature and hypothesized variation in coefficient of friction. In a later section, the relation between wall temperature and friction will be treated in more detail.

Deposition by Impact of Large Particles

Large particles may be formed in the combustor as a result of poor fuel sprays, or as coke-like deposits that break away from engine surfaces. In the case of solid-propellant rockets, it may be caused by nothing more than unglamorous disintegration of the fuel charge. Particles from these origins are difficult to classify.

Types of particles that respond to a slightly more analytical definition are those that start their existence as submicron particles, diffuse to walls, form liquid films, and finally form drops as the films are dispersed back into the gas stream.

Reasonable approximations can be made of the size and number of particles formed by this process in a number of cases. An example is the surface of a combustor exposed to a condensable vapor. The amount of liquid collecting on the surface can be calculated by mass transfer relations of the type previously discussed. If the surface terminates in the gas stream, the liquid film must enter the gas stream. During the process of entering, the high velocity gas will tend to break up the film. The interaction forces are simply those of the liquid atomization processes. Atomization is comprehensively treated in the literature (ref. 40) and so will not be reviewed in detail herein. Applications of the more comprehensive equations allow the estimate of drop size and size distribution for liquids of various physical properties. Analysis for particles generated by atomization of liquid films from engine surfaces indicate that most would be larger than 10 microns.

Information on the particle size, mass, and concentration of these larger drops can be used to predict deposition rates due to particle impingement. The subject of particle impingement is thoroughly covered in the literature, largely motivated by aircraft icing problems. Recently, work has appeared directed towards the solution of turbine fouling, for example, publications by Smith[35], Martlew[41], and Hodge[42].

The common starting point for all impingement studies is the equations of motion of a particle in a moving gas stream.

These equations of motion for a two-dimensional case or for a body in axisymmetric flow are identical and may be expressed as

$$\frac{dV_z}{d\tau} = \frac{C_D Re}{24} \frac{1}{K} (u_z - V_z) \tag{38}$$

$$\frac{dV_r}{d\tau} = \frac{C_D Re}{24} \frac{1}{K} (u_r - V_r) \tag{39}$$

where

K $\frac{2}{9} \frac{\rho r^2 u}{\mu l}$

C_D drag coefficient for drops

V_z axial velocity, ratio of actual droplet velocity to free-stream velocity, dimensionless

V_r corresponding velocity ratio perpendicular to axis of flow

u local air velocity ratio referred to free stream

V local droplet velocity referred to free stream

U free-stream velocity

ρ droplet density

l characteristic dimension of obstruction to flow

The equations are often written in the dimensionless form just shown to make the results more general. The coefficient of drag varies; so that tabulated values for spheres, such as appear in reference 43, are often used. The Stokes law value applies as relative velocity approaches zero.

The solution of the equations is difficult because terms such as velocity components and coefficient of drag are inextricably entwined. The procedures employed often involve step-by-step analysis of the particle motion in the particular flow field in question. Solution may be accelerated by the use of differential analyzers. One such differential analyzer used in droplet trajectories studies is discussed in reference 44. Even with the aid of the mechanical gadgetry, simplifying assumptions must be made to keep the problem within reasonable bounds. The usual assumptions are:

(1) The droplets move at the same velocity as the gas ahead of the distorted flow field.

(2) The droplets can be treated as spheres and do not change with size.

(3) Gravitational forces are negligible.

Many solutions of the droplet trajectories have been completed. Martlew(41) presents theoretical and experimental results for a turbine cascade. Members of the Lewis Research Center have completed solutions for many of the particle sizes, flow conditions (pressure, temperature, and velocity) and flow fields of interest. Some of the flow fields explored are those around rectangular half bodies (ref. 45), cylinders (ref. 44), spheres (ref. 46), several ellipsoids (refs. 47 and 48), 60° and 90° elbows (refs. 49 and 50), and various airfoil shapes (refs. 51 and 52). In the large number of flow fields treated, almost all probable internal flows have been approached to a degree of accuracy commensurate with the accuracy of the other variables in the study of deposition. If desired, it is possible to synthesize additional flow fields by superposing parts of existing solutions.

A typical set of impingement data for a cylinder from reference 44 is shown in the next three figures. The flow field of the cylinder is shown in figure 7.

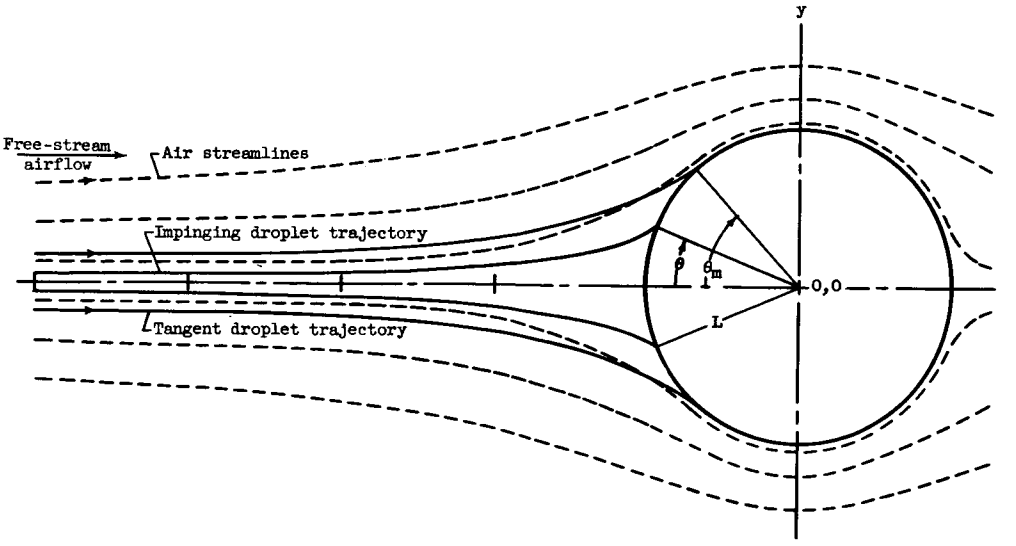

Figure 7. - Air streamline and droplet trajectories with respect to right circular cylinder.

Typical droplet trajectories at a free-stream Reynolds number of 63.246, inertia parameter, $(K=2,\rho_l r^2 u/\mu l)$, and φ (generalized flow parameter, Re_0^2/K) of 1000 are shown in figure 8.

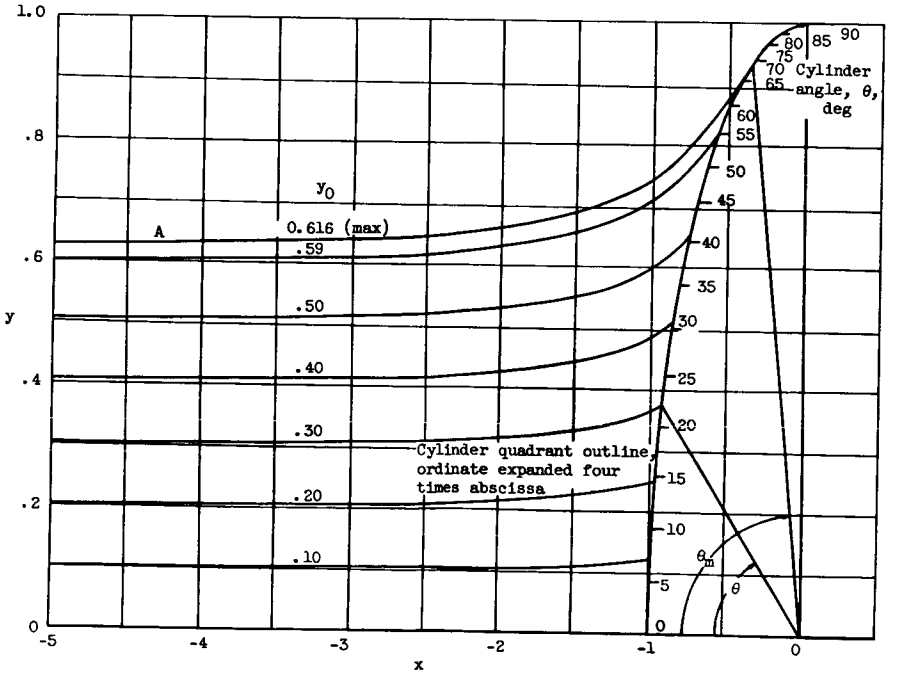

Figure 8. - Trajectories of droplets impinging on cylinder. Free-stream Reynolds number, 63.246; inertia parameter, 4; φ, 1000.

The results integrated for the entire cylinder result in a collection efficiency for the cylinder. A typical result is shown in figure 9, where φ is the flow parameter and K is the inertia parameter previously defined.

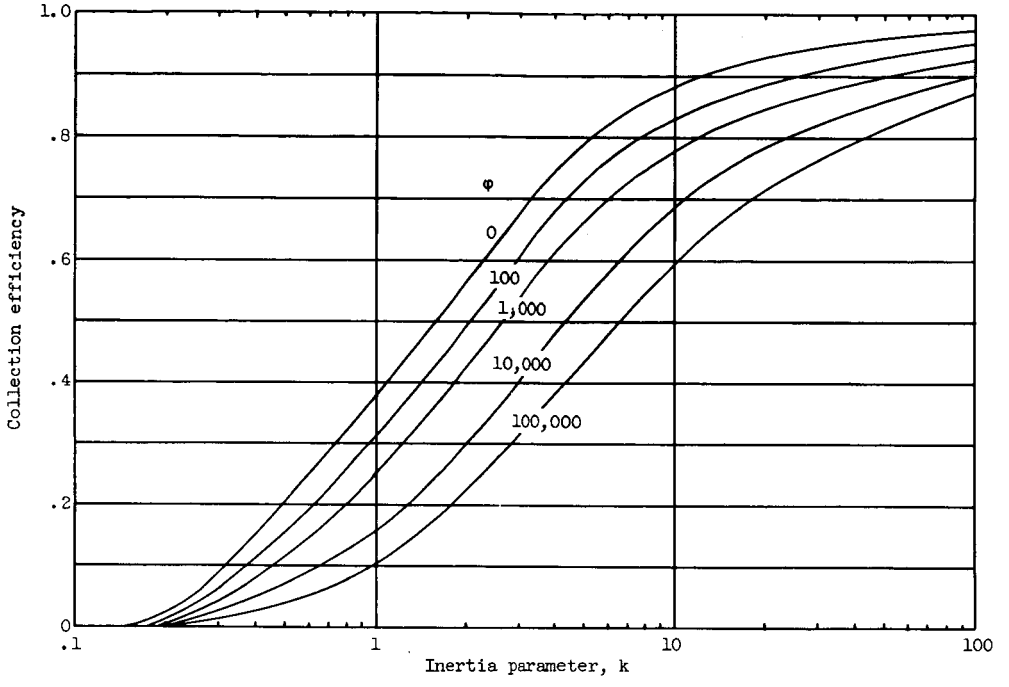

Figure 9. - Cylinder collection efficiency.

Quite accurate estimates of droplet impingement are available by use of the preceding data; but, if a variety of shapes are to be treated, the method requires a fairly large stockpile of references. Approximate solutions of trajectory calculations exist; one such method is discussed by Smith(35). Smith, following the lead of G. I. Taylor, defines an impact number I'. If I' is less than 1/8, the particle escapes the surface; I', expressed for the potential flow field normal to a cylinder at the stagnation point, is

$$I = \frac{2}{9} \frac{\rho_p}{\rho_v} \left(\frac{r_p}{r_{cylinder}} \right)^2 (Re) \qquad (40)$$

where the Reynolds number is based on the radius of the cylinders.

Limitations of impingement studies. - The effect of compressible flow on droplet trajectories has been examined in reference 53. Little effect is noted at velocities up to critical; the small changes of compressible flow do not warrant the additional effort. Most of the work on droplet trajectories was based on

water, which has a relatively high surface tension; thus, droplet shattering usually has been neglected. However, for particles whose cohesive forces are small, the effect of the dynamic forces experienced by the drop as it intercepts flow streamlines should be at least cursorily examined to see if conditions of particle shattering exist.

Summary Remarks on Deposition

Examination of the relations in figure 9 or the use of equation (36), although they do not agree exactly, do point out that particles less than 1×10^{-4} centimeter (1 micron) will not collect, because of impingement. On the other hand, the diffusion relations indicate very slow rates of deposition in laminar flow for particles that approach the 1 micron size. Deposition rate expressions exist for particles in turbulent flow for Schmidt numbers up to 3000 and for Schmidt numbers greater than 10^5. The turbulent mass transfer relations apparently respond to the general similitude relations and indicate significant deposits may form at jet engine conditions.

DEPOSIT THICKNESS

Liquid Film Thickness

Thickness of liquid films with concurrent gas flow has been calculated by Abramson(54) on the basis of simultaneous solution of boundary-layer equations of the liquid and gas flow. The method employed by Abramson was to note that the pressure drop per unit length in the gas must be equal to the pressure drop of a fictitious continuation of the liquid film. Appropriate values of friction factors were used for both gas and liquid. In essence, it was stipulated that at the liquid-gas phase boundary, the shear stress was equal for the two fluids. The final equation for the film thickness was

$$t_l = y_l^+ \frac{u_l}{\sqrt{\rho_l}} \sqrt{\frac{2}{C_f \rho_v u_v^2}} \tag{41}$$

where

$$y_l^+ = \frac{\sqrt{\tau_0' \rho_0}}{\mu_0 / \rho_0} y$$

the quantity y^+ is a dimensionless boundary-layer parameter (see ref. 55). The parameter was evaluated by Abramson as a function of liquid flow rate, wetted perimeter, and viscosity; the results appear in graphical form in reference 54.

A similar expression for thickness of liquids has been suggested by Setze(56). His expression again equates shear stress at the liquid-gas interface, but the analytical expression is

simplified by the assumption of a linear velocity profile in the liquid film.

$$\tau_v' = C_f \frac{\rho_o u_o^2}{2g}$$

$$\tau_l' = \frac{\mu}{g}\left(\frac{du}{dy}\right) = \frac{\mu}{g}\left(\frac{u_l}{t_l}\right)$$

Application of the continuity equation for the linear velocity gradient results in

$$t_l = \sqrt{\frac{2\dot{w}_l \mu_l}{C_f \rho_o u_o^2 \rho_l}} \qquad (42)$$

where $\dot{w}_l$ is rate of liquid flow.

Setze treated only the case of turbulent gas stream and laminar liquid films. It would appear that reasonable approximations could be made of the laminar gas stream - laminar film and turbulent gas stream - turbulent liquid film if the appropriate C_f is used. The assumption of linear velocity gradient for a turbulent film would probably indicate a film slightly thicker than actuality.

Stability of Liquid Films

It is of interest to estimate when liquid films become turbulent, since the onset of turbulent disturbances in the liquid film increases frictional losses. This change in liquid film properties was noted by Abramson(54), who estimated the transition to turbulent liquid flow was accompanied by a 2-to-4-fold increase in frictional losses.

The transition to turbulent liquid flow occurs when the flow rate of the liquid is sufficient to increase the liquid film thickness to the point where turbulent forces predominate over the viscous forces.

The conditions for smooth laminar liquid films, using the approach of Abramson(54), at $y^+ \approx 12$ (y^+ is defined in eq. (41); disturbances appear at values of y^+ between 12 to 21; above 21 the film becomes progressively more turbulent.

An approximate method of defining the condition of flow transition is suggested by Knuth(57). If the normal velocity gradient in the liquid film is assumed constant as in equation (42), the dimensionless stability parameter t' (see ref. 58) may be calculated from

$$t' = \sqrt{\frac{2\dot{w}_l}{g'\mu_l}}$$

When t' is greater than 30, the flow should be assumed turbulent. These equations assumed liquid viscosity was constant through the film. Solutions exist for variable viscosity (ref. 57).

The interdependence of flow stability, film thickness, and coefficient requires iterative solutions for flow near the transition point. Unfortunately, the variation of C_f with transition into turbulent flow is not well known.

Mixed Phase Deposit Thickness

Solids suspended in liquid films may greatly affect the flow behavior of viscous liquid films. One of the more obvious examples is the large particles lodged in a viscous film. If a temperature gradient exists in the film, then the large particles communicate the high flow resistance of the cooler fluid into the main gas streams.

Interesting effects have been observed in that apparently trace amounts of some solids exhibit a large effect in increasing or decreasing viscosity of some fluids films.

Thickness of Solid Deposits

The thickness of solids cannot be predicted with any degree of accuracy. Most of the solid deposit work is highly qualitative.

Some evidence exists to indicate that solids formed in the gas stream do not in themselves form surface deposits. The gas-borne solids deposit only when liquids bind them to surfaces.

Support for this point of view is the observation of the small attractive forces of "dry" particles for solid surfaces. Also, experimental work on combustion of magnesium is in accord with the low "sticking probability." Ramjet engines were operated with magnesium slurries that produced about 1/8 pound of magnesium oxide per pound of air. When the combustion efficiency was high, only traces of deposits were noted on exit nozzle surfaces. The deposits in the engine usually appeared to be caused by traces of unburned molten magnesium metal.

EFFECTS OF DEPOSITS

The effect of deposition on component performance can be approached by relating the deposition effect to the effect of surface roughness on skin friction drag and the effect of roughness on transition from laminar to turbulent flow. Many excellent articles exist in this field. Convenient summary articles are also available on both these subjects, for example, Clauser's[59] paper on the turbulent boundary layer and Dryden's[60] review of

the effect of roughness on boundary-layer transition. A recent study by Goddard(61) indicates that, for roughness sizes where the quadratic resistance law holds, the skin friction drag is a simple function of the roughness Reynolds number at speeds up to a Mach number of 5, the same as in the incompressible-flow case.

Thus, if the deposits result in moderately well distributed surface roughness, the frictional losses can be accurately calculated from the subsonic surfaces of the combustor to the surfaces exposed to supersonic velocities in the exhaust nozzle.

At times the deposits will penetrate through the boundary layer. When this occurs, the usual surface roughness Reynolds number functions cannot be used. At these conditions, wave drags will be encountered and may be quite large at supersonic flow conditions.

An examples of the losses in stream thrust caused by deposits on surfaces exposed to supersonic flow are shown in figure 10.

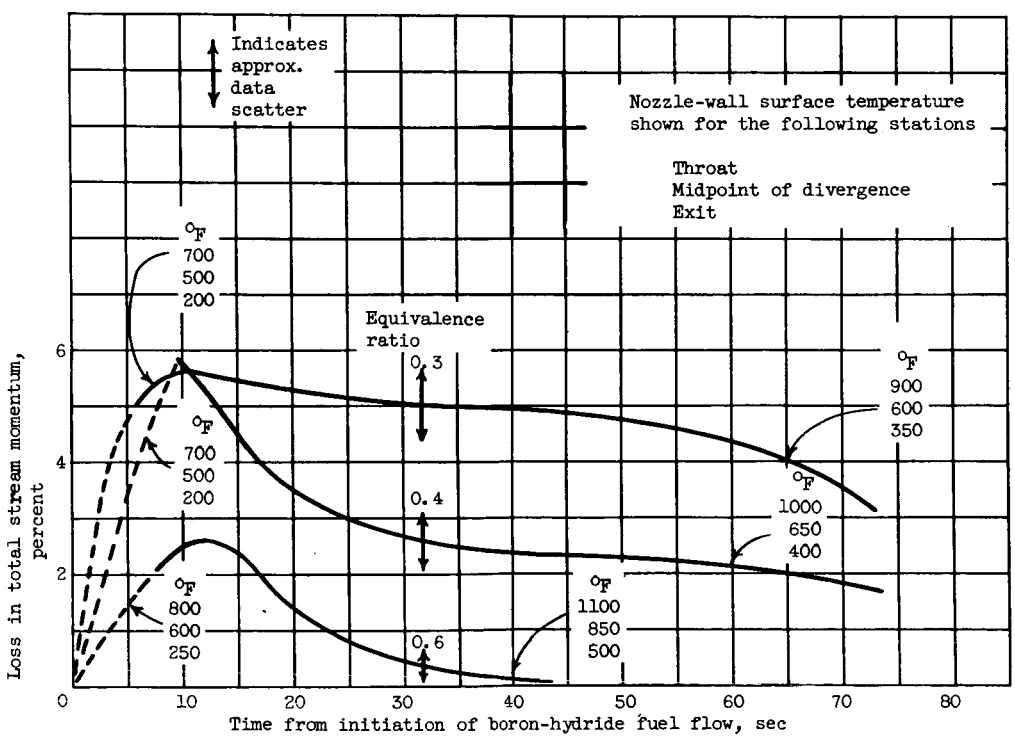

Figure 10. - The effect of boric oxide deposits on the performance of a convergent-divergent nozzle.

The deposits resulted from deposition of boric oxide on the surfaces of a convergent-divergent nozzle. It was established that the loss was primarily due to drag on the divergent (supersonic) part of the nozzle. Quantitative control of the amount and

characteristic of the deposit was not maintained, but some trends can be observed.

The time history of three tests is shown. These test differred in fuel-air ratio of the boron-containing fuel. The high-temperature test also had the highest boric oxide concentration in the gas stream. The losses in stream momentum appeared to be completely dominated by the surface temperatures of the nozzle. In order to relate surface temperature to viscosity of boric oxide and thus relative thickness of deposit, a few representative values of viscosity are listed:

Temperature, °F	Boric oxide viscosity, poise
1400	3,500
1200	12,000
1000	60,000
800	300,000

Examination of the frictional losses of the low wall-temperature data indicated that surface roughness was probably producing a form of wave drag.

Similar tests have been conducted in studies of flow through turbine nozzles. An example is reference 62, wherein measurement was made of losses due to fouling of turbine stator blades by fuel ash. The results indicated a direct correlation of cascade performance loss with operating time and with mass of fuel burned when the blade temperatures were below the solidification point of the fuel ash. The losses increased rapidly with deposit weight and amounted to a 35-percent drop in discharge coefficient at the end of a 20-hour test. High efficiencies could be maintained if the blades were operated above the melting point of the fuel ash.

Predictable effects of deposits on engine performance include flow of viscous liquids through nozzles. The change in throat areas can be analytically predicted by equations such as (42) if: (1) The upstream conditions are such as to permit a reasonable estimate of mass flow rate of the film, and (2) the viscosity of the liquid film is known.

An interesting effect of viscous liquid films is the tendency to collect in separate flow regions. The kinetic forces tending to remove the film are markedly reduced (eqs. (41) or (42)) and thus the viscous deposits accumulate. If an adverse pressure gradient exists in the boundary layer, these deposits may tend to move upstream and cause a larger disturbance to flow.

Losses of performance in rocket engines are difficult to present, since the results are often catastropic. The deposits apparently affect fuel spray patterns, producing the serious performance losses.

In general, perhaps the most severe losses caused by deposits are those interfering with combustor performance. Small traces of deposits can alter fuel spray patterns, which may in turn accelerate new deposits and thus establish a pathway to engine failure.

CONCLUDING REMARKS

An attempt has been made to enumerate some of the factors leading to deposits in jet engines and to briefly illustrate some of the consequences of their existence. The approach used in developing the relations relating to the cause and effect of deposits and possible cures was, of course, prejudiced by the author's immediate experiences. It is hoped, however, that some light has been cast on the understanding, or in some cases the lack of understanding, of the physical steps leading to formation of the surface residues.

SYMBOLS

A	area
a	growth rate constant
b'	Reichart b' function
C	constant
C_D	coefficient of drag
C_f	coefficient of friction
D	diameter
$\mathscr{D}$	diffusion coefficient
F	free energy of particle
f	function
g	number of particles or molecules
h	heat transfer coefficient
$h_{\mathscr{D}}$	mass transfer coefficient
I	droplet formation rate
I'	impact parameter
K	a constant, or an inertia parameter
k	Boltzmann constant
L	mean free path
$\mathscr{L}$	heat of vaporization
l	length
M	molecular weight
m	mass of molecule
N_l	number of liquid molecules
N_v	number of vapor molecules
n	number of particles per unit volume
Pr	Prandtl number
p	pressure
Re	Reynolds number

r	radius
S	sum of effective diameters
Sc	Schmidt number
Sh	Sherwood number
St	Stanton number
T	temperature
t	thickness
u	velocity
v'	dimensionless velocity
V	volume
V_l'	volume of one molecule in liquid phase
v	velocity
w	mass flux
$\dot{w}$	weight flow rate
x	mole fraction
y	dimension
β	molecular collision term
θ	number of collisions
λ	thermal conductivity
μ	viscosity
υ	number of constituents
ρ	density
σ	surface tension
τ	time
τ'	shear stress
Ψ	collision frequency function

Subscripts:

0	reference state, original state

1,2,3	number of molecules or constituents
∞	infinity
g	number of particles or molecules
l	liquid
P	particles
r	normal or radial direction
v	vapor
z	dimension

Superscript:

*	critical particle

REFERENCES

1. Breitwieser, R., Gordon, S., and Gammon, B.: Summary Report on Analytical Evaluation of Air and Fuel Specific-Impulse Characteristics of Several Nonhydrocarbon Jet-Engine Fuels. NACA RM E52L08, 1953.

2. Olson, W. T., and Setze, P. C.: Some Combustion Problems of High Energy Fuels for Aircraft. Paper presented at Seventh International Symposium on Combustion, Oxford Univ., (England), Aug. 28, 1958.

3. Stull, D. R.: Vapor Pressures of Inorganic Compounds, up to 1 Atmosphere. Ind. and Eng. Chem., vol. 39, 1947, p. 517.

4. Setze, P. C.: A Review of the Physical and Thermodynamic Properties of Boric Oxide. NACA RM E57B14, 1957.

5. Perry, J. H., ed.: Chemical Engineers' Handbook. Third ed., McGraw-Hill Book Co., Inc., 1950.

6. Frenkel, J.: Kinetic Theory of Liquids. Dover Publ., 1955, pp. 368-400.

7. Stever, H. G.: Condensation Phenomena in High Speed Flows. Fundamentals of Gas Dynamics, High Speed Aero. and Jet Prop., Princeton Univ. Press, 1958, pp. 536-548; 564-572.

8. von Helmholtz, R.: Ann. Phys., 27, 1886.

9. Gibbs, J. W.: Collected Works. Longmans, Green and Co., 1931.

10. Thomson, W.: Proc. Roy. Soc., Edinburgh VII, 1870, pp. 63-68.

11. Volmer, Max: Kinetik der Phasenbildung. Theodor Steinkopf (Dresden und Leipzig), 1939.

12. Becker, R., and Döring, W.: Kinetische Behandlung der Keimbildung in Übersättigten Dampfen. Annalen der Phys., Bd. 24, 1935, pp. 719-752.

13. Zeldovich, Y. B.: Jour. Exp. and Theoretical Phys., U.S.S.R., 12, 1942, pp. 525-538.

14. Oswatitsch, K. Z.: Angew. Math. u. Mech., 22, 1942, pp. 1-14.

15. Kantrowitz, A.: Nucleation in Very Rapid Expansions. Jour. Chem. Phys., vol. 19, no. 9, Sept. 1951.

16. Probstein, R.: Time Lag in the Self-Nucleation of a Supersaturated Vapor. Rep. 168, Aero. Eng. Lab., Princeton Univ., Nov. 27, 1950.

17. Setze, P. C.: A Study of Liquid Boric Oxide Particle Growth Rates in a Gas Stream from a Simulated Jet Engine Combustor. NACA RM E55I20a, 1957.

18. Collins, F. C.: Time Lag in Spontaneous Nucleation Due to Non-Steady State Effects. Zs. f. Elecktrochemie, 1955, pp. 404-407.

19. Head, R.: Ph.D. Thesis, Guggenheim Aero. Lab., C.I.T., 1949.

20. Tolman, R. C.: Jour. Chem. Phys., 17, 1949, pp. 333-337.

21. Bogdonoff, S. M., and Lees, L.: Study of the Condensation of the Components of Air in Supersonic Wind Tunnels. Rep. 146, Aero. Eng. Lab., Princeton Univ., 1949.

22. Reed, S. G., Jr.: On Early Stages of Condensation. Ph.D. Thesis, Catholic Univ. of America, 1951.

23. Jeans, J. H.: Kinetic Theory of Gases. Cambridge Univ. Press, 1940, pp. 130-140.

24. Langstroth, G. O., and Gillespie, T.: Coagulation and Surface Losses in Disperse Systems in Still and Turbulent Air. Canadian Jour. Res., vol. 25, sec. B, 1947, pp. 455-471.

25. Arthur, P. D., and Nagamatsu, H. T.: Effects of Impurities on the Supersaturation of Nitrogen in a Hypersonic Nozzle. Hypersonic Wind Tunnel Memo. 7, GALCIT, Mar. 1952.

26. Schalla, R. L., and Hibbard, R. R.: Smoke and Coke Formation in the Combustion of Hydrocarbon-Air Mixtures. Ch. IX of Basic Considerations in the Combustion of Hydrocarbon Fuels with Air. NACA Rep. 1300, 1957.

27. Clark, Thomas P.: Examination of Smoke and Carbon from Turbojet-Engine Combustors. NACA RM E52I26, 1952.

28. Brokaw, R. S.: Unpublished NASA Notes on Transport Properties.

29. Hirschfelder, J. O., Curtiss, C. F., and Bird, R. B.: Molecular Theory of Gases and Liquids. John Wiley & Sons, Inc., 1954.

30. Hirschfelder, J. O., and Curtiss, C. F.: Third Symposium on Combustion and Flame and Explosion Phenomena, The Williams & Wilkins Co., Baltimore, 1949, p. 124.

31. Buddenberg, J. W., and Wilke, C. R.: Ind. and Eng. Chem., vol. 41, 1949, p. 1345.

32. von Kármán, Th.: Fundamental Equations in Aerothermochemistry. Selected Combustion Problems, II, AGARD, Butterworths Sci. Pub. (London), 1956.

33. Chapman, S.: Thermal Diffusion in Gases, Transport Properties in Gases. Gas Dynamics Symposium, Northwestern Univ. Press, 1958.

34. Cawood, W.: Trans. of Faraday Soc., vol. 32, 1936, p. 1068.

35. Smith, M. C. G.: A Theoretical Note on the Mechanism of Deposition in Turbine Blade Fouling. Memo. 145, British N.G.T.E., 1952.

36. Eckert, E. R. G.: Introduction to the Transfer of Heat and Mass. McGraw-Hill Book Co., Inc., 1950, pp. 249-251.

37. Reichardt, H.: Fundamentals of Turbulent Heat Transfer. NACA TM 1408, 1957. (Trans. from Archiv. f. die Gesamte Warmetechnik, no. 617, 1951.)

38. Metzner, A. B., and Friend, W. L.: Theoretical Analogies Between Heat Mass Momentum Transfer and Modifications for Fluids of High Prandtl or Schmidt Numbers. Canadian Jour. Chem. Eng., vol. 36, 6; 1958, p. 235.

39. Setze, P. C.: Unpublished data on Boric Oxide Deposition.

40. Anon.: The Penn State Bibliography on Sprays. Second ed., The Texas Co. (N.Y.), Dec. 1953.

41. Martlew, D. L.: The Distribution of Impacted Particles of Various Sizes on the Blades of a Turbine Cascade. Memo. 274, British N.G.T.E., Oct. 1956.

42. Hodge, R. I.: The Fouling of Turbine Blading by the Products of Combustion of Pulverized Fuel, Part IV. Memo. 253, British N.G.T.E., 1955.

43. Bergrun, N. R.: A Method for Numerically Calculating the Area and Distribution of Water Impingement on the Leading Edge of an Airfoil in a Cloud. NACA TN 1397, 1947.

44. Brun, R. J., and Mergler, H. W.: Impingement of Water Droplets on a Cylinder in an Incompressible Flow Field and Evaluation of Rotating Multicylinder Method for Measurement of Droplet-Size Distribution, Volume-Median Size, and Liquid-Water Content in Clouds. NACA TN 2904, 1953.

45. Lewis, W., and Brun, R. J.: Impingement of Water Droplets on a Rectangular Half Body in a Two-Dimensional Incompressible Flow Field. NACA TN 3658, 1956.

46. Dorsch, R. G., Saper, P. G., and Kadow, C. F.: Impingement of Water Droplets on a Sphere. NACA TN 3587, 1955.

47. Dorsch, R. G., Brun, R. J., and Gregg, J. L.: Impingement of Water Droplets on an Ellipsoid with Fineness Ratio 5 in Axisymmetric Flow. NACA TN 3099, 1954.

48. Brun, R. J., and Dorsch, R. G.: Variation of Local Liquid-Water Concentration about an Ellipsoid of Fineness Ratio 10 Moving in a Droplet Field. NACA TN 3410, 1955.

49. Hacker, P. T., Brun, R. J., and Boyd, B.: Impingement of Droplets in 90° Elbows with Potential Flow. NACA TN 2999, 1953.

50. Hacker, P. T., Saper, P. G., and Kadow, C. F.: Impingement of Droplets in 60° Elbows with Potential Flow. NACA TN 3770, 1956.

51. Brun, R. J., and Vogt, D. E.: Impingement of Water Droplets on NACA 65A004 Airfoil at 0° Angle of Attack. NACA TN 3586, 1955.

52. Brun, R. J., Serafini, J. S., and Moshos, G. J.: Impingement of Water Droplets on an NACA 65_1-212 Airfoil at an Angle of Attack of 4°. NACA RM E52B12, 1952.

53. Brun, R. J., Serafini, J. S., and Gallagher, H. M.: Impingement of Cloud Droplets on Aerodynamic Bodies as Affected by Compressibility of Air Flow Around the Body. NACA TN 2903, 1953.

54. Ambramson, A. E.: Investigation of Annular Liquid Flow with Cocurrent Air Flow in Horizontal Tubes. Jour. Appl. Mech. 52-APM-11.

55. von Kármán, Th.: The Analogy Between Fluid Friction and Heat Transfer. Trans. ASME, vol. 61, no. 8, Nov. 1939, pp. 705-710.

56. Setze, P. C.: Unpublished note on Equilibrium Thickness of Boric Oxide.

57. Knuth, E. L.: A Study of the Mechanics of Liquid Films as Applied to Film Cooling. Prog. Rep. 1-79, J.P.L., 1951.

58. McAdams, W. H.: Heat Transmission. McGraw-Hill Book Co., Inc., 1942, pp. 109-110.

59. Clauser, F. H.: The Turbulent Boundary Layer. Advances in Appl. Mech., vol. IV. Academic Press, Inc., 1956.

60. Dryden, H. L.: Review of Published Data on the Effect of Roughness on Transition from Laminar to Turbulent Flow. Jour. Aero. Sci., vol. 20, no. 7, July 1953, pp. 477-482.

61. Goddard, F. E., Jr.: Effect of Uniformily Distributed Roughness on Turbulent Skin-Friction Drag at Supersonic Speeds. Jour. Aero/Space Sci., vol. 26, no. 1, Jan. 1959, pp. 1-15.

62. Macfarlane, J. J., and Whitcher, F. S. E.: The Fouling of Turbine Blades by Fuel Ash. Part VI. Pressure Tests with Cambered Blades. Memo. R.193, British N.G.T.E., July 1956.